In situ Printing – An Alternative Three Dimensional Laden Structure Fabrication Method

Y. Liu[1], W. Sun[1, 2, 3, 4]

[1] Department of Mechanical Engineering, Drexel University, Philadelphia, PA, USA
[2] Department of Mechanical Engineering, Biomanufacturing Center, Tsinghua University, Beijing, People's Republic of China
[3] Biomanufacturing and Rapid Forming Technology Key Laboratory of Beijing, Beijing, People's Republic of China
[4] Biomanufacturing Engineering Laboratory, Shenzhen Tsinghua Graduate School, Shenzhen, People's Republic of China

Email: weisun@drexel.edu and weisun@tsinghua.edu.cn

REVIEWED

Abstract

Recapitulating a structure that mimics the anatomic geometries and intratissue cell distribution as in live organism is a major challenge of tissue engineering nowadays. Solid free-form fabrication (SFF) has been demonstrated as an efficient tool for this purpose. In this paper we presented a SFF based *in situ* printing method that is free of fabrication time frame and fabrication environment constrains. The fabrication parameters on strut formability, fabricated structural stability against gentle fluidic disturbance, and the integrity of the fabricated structure in cell culture environment were studied to assess the potential of the fabrication method on biomedical application. Based on the results, controlled strut formability can be achieved in an appropriate cross-linking deposition range. Alginate composition is the main parameter that dominates the stability and integrity of the fabricated structure. A parameter set that can produce a stable scaffold with the ability to maintain its structure in cell culture environment for at least 15 days was optimized.

Introduction

Tissue engineering is an interdisciplinary realm that utilizes engineering and life science principles to advance the knowledge of tissue growth and behavior, which can be applied further toward the development of biological substitutes that restore, maintain, or improve tissue function. [1] Native tissue architectures are highly hierarchical in three-dimensional (3D) with heterogeneous cells and bioactive factors in precise disposition. This spacious allocation is found critical to tissue growth and function. Thus, it is a major challenge in tissue engineering nowadays to recapitulate the structures that mimic the anatomic geometries and intratissue cell distribution. A famous pioneering work by Charles Vancanti and colleagues has demonstrated the therapeutic promise in which tissue-engineered cartilage was formed into human ear shape. [2] Similar cartilage structure was further extended to temporomandibular disc [3] and joint, [4] meniscus, [5] trachea, [6] intervertebral disc, [7] nasal tip, [8] and nasal septum, [9] as well as other bone structures as femoral shaft, [10] mandibular condyle [4] and distal phalanx. [11]

While complex shapes were created, those technologies still lack the ability to incorporate cells and bioactive components to create a cellular spatial heterogeneities within the construct. To overcome this drawback, cell printing methods was introduced in tissue

engineering to deliver an efficient method for fabricating 3D laden structure within which versatile distribution of heterogeneous cells can be achieved. To fabricate 3D laden structure incorporating bioactive components, various tools, such as inkjet [12, 13], laser-guided printing [14], two-photon polymerization and laser induced forward transfer [15], and 3D bioactive solid free-form fabrication [16-20], have been developed. Solid free-form fabrication (SFF) technology, often referred to as rapid prototyping, is analogous to 3D printing. In general, materials were fabricated and guided into different patterns for each layer, and subsequent layers were fused to build a complete free-form geometry. 3D bioactive SFF has been demonstrated high efficiency to build structure with complex geometries, as well to incorporate and maintain high viability of cells and activities of other bioactive component during the fabrication process.

Various 3D bioactive SFF technologies have been explored to build 3D laden structures with cells encapsulated. Cohen et al developed a direct SFF technology where alginate was mixed with $CaSO_4$ in advance as deposition material.[16] The pre cross-linked hydrogel was then mixed with cells and extruded for fabrication. Ahn et al modified this technology by introducing an aerosol cross-linking process.[17] In this method, alginate mixed with cells was pre cross-linked with $CaCl_2$ and extruded for printing. During the printing process, an additional $CaCl_2$ solution was fumed with ultrasonic humidifier constantly flowing on the fabrication stage for further solidification. Khalil et al utilized an alternative method for cross-linking solidification.[18] They mixed the alginate solution with cells and extruded to reservoir where a $CaCl_2$ solution with a depth same as the deposition layer thickness had been deposited for cross-linking. For each of the layer build up, $CaCl_2$ solution was deposited in advance to elevate the solution level for another layer thickness. In addition to ionic cross-linking, temperature controlling system was also introduced to assist solidification. Ahn et al developed a direct cell printing supplemented with low- temperature processing method.[19] In the dispensing process, alginate was mixed with cell-freezer solution and then mixed with cells as cell delivery material. The deposition material was extruded while a cooling system was circulating to cool the dispenser and working stage to solidify the extruded material. Fabricated scaffold was subsequently cross-linked with $CaCl_2$. Zhao et al also utilized temperature controlled system for 3D cellular laden structure fabrication.[20] In their study, gelatin/alginate/fibrinogen hydrogel was used as cell delivery material and pre-mixed with cells. The deposition material was loaded to a temperature controlled deposition system where temperature was maintained as 25 ^{0}C before extrusion and 10 ^{0}C after extrusion. This temperature difference dominates the solidifying process of the gelatin and thus delivers a porous scaffold structure with cells incorporated. Though the previous technologies have been demonstrated high cell viability and potential for cell proliferation, there are some limitations. The pre cross-linked alginate utilized a time dependent solidification process thus is constrained in a specific fabrication time frame. Reservoir crosslinking method is constrained by the topology of the reservoir and the scale size of the scaffold. Temperature control system requires an additional power supply and a specific working stage that limited the system's portability.

We presented an alternative fabrication method that is not constrained by a fabrication time frame, nor requires a specific printing stage or an additional power supply. A dual-nozzle system was utilized as deposition tool that mounted on the 3D motion system. In the dual-nozzle system, cell delivery material alginate and cross-linker material $CaCl_2$ were loaded on each of the nozzle. The dual-nozzle extrusion tips were brought together for an *in situ* cross-linking process to fabricate 3D laden strut. Struts were designed and guided by the motion system to

fabricate a complete 3D laden porous scaffold. This paper reports on our preliminary study of *in situ* printing technology and the parametric characterization of the system on developing 3D porous laden structure. Deposition material was extruded and *in situ* cross-linked with variant fabrication parameters into struts which were guided to multiple layers stacked together as scaffold. The strut formability, fabricated structural stability against gentle fluidic disturbance, and the integrity of the fabricated structure in cell culture environment were studied to assess the potential of the fabrication method on biomedical application.

Materials and Methods

Cell-dispensing system

A proprietary 3D bio-printer was developed in this study to fabricate 3D laden structure. The 3D bio-printer includes a CAD/CAM integrated 3D motion system and a multi-nozzle biopolymer deposition system. The motion system was composed by three orthogonal robotic arms that move the loaded deposition nozzles in a 3D pre-defined pathway. The path can be programmed using an in- house software that is designed for CAD models. A CAD scaffold model that imported was first converted into STL format, and then sliced into multiple layers for toolpath generation. The path file was then imported to the motion system for freeform fabrication with variant motion parameters controllable. The motion resolution is 10 μm in the three orthogonal directions and has minimum velocity of 100 μm/ s.

The multi-nozzle deposition system is mounted on the 3D motion system. Each nozzle deposition system consists of an air pressure supply, a material delivery tube, a dispensing nozzle system with pneumatic control, and a replaceable needle tip. Deposition solutions were loaded in material delivery tube. The solution in material delivery tube is driven by a controllable air supply for flow rate control and continues with a dispensing nozzle system that is digitally controllable for turning on and off by a pneumatic control supply. The digital switch is integrated to PC and is coordinated to the motion system while 3D fabricating. The deposition solution goes through the dispensing nozzle system is finally extruded out through the interchangeable needle tip. Breathing air (Airgas) was used for air supply with high precision air pressure regulator for flow rate tuning. The *in situ* printing technology requires a dual nozzle system with the dispensing tip positioned together for immediate cross-linking. The dual nozzle system was loaded with deposition material (alginate) and cross-link material (calcium chloride) respectively. During the fabrication, appropriate amount of solutions are extruded and quick cross-linking of the deposition material occurred to form the gel strut.

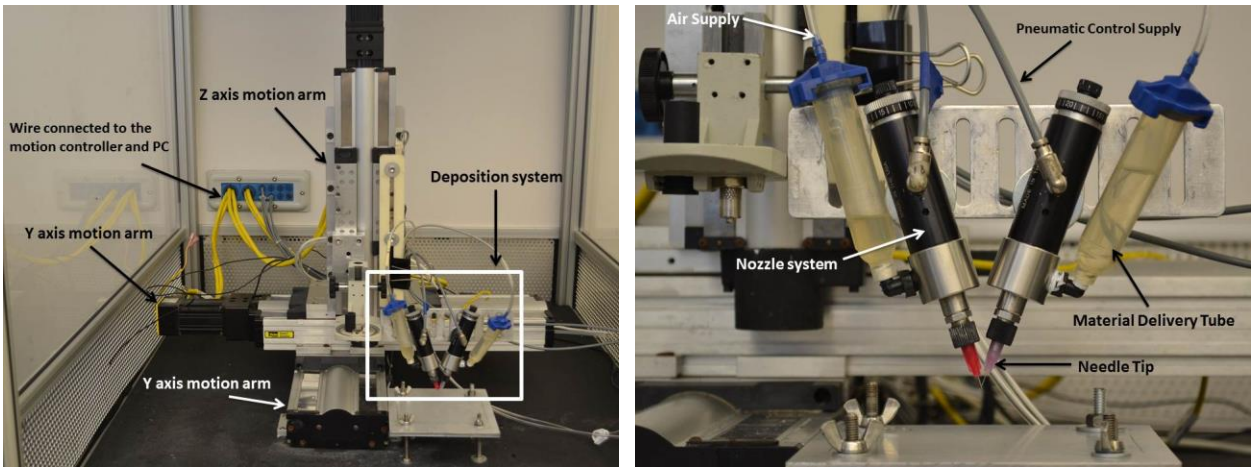

Figure 1. 3D bio-printer system and multi-nozzle deposition system

Chemical formulation

Alginic acid sodium salt from brown algae with low viscosity and low glucuronic acid content (A0682, Sigma), and the product with medium viscosity and high glucuronic acid content (71238, Sigma) were selected as deposition material for this study. Those alginate products and their mixtures were dissolved in deionized (DI) water at various concentrations and left magnetic stirred overnight to ensure homogeneity and consistent viscosity. An ionic cross-linking solution was prepared by dissolving calcium chloride (ACS grade anhydrous, amresco) in DI water at various concentrations. DPBS, 1X (Dulbecco's Phosphate Buffered Saline) was used for scaffolds rinse.

Strut formability

The strut formability of *in situ* printing was examined by measuring the extruded solidified strut size and comparing it with expected strut size. An analytic model was developed to determine the expected strut size. The analytic model was developed based on the assumption that the alginate is cross-linked within a certain time frame when being extruded out thus deliver a cylindrical gel strut and limited swollen occurred, the diameter of the strut (D) can be expressed as a function of the fluid rate (Q), and the speed of the nozzle movement (v): $D = f(Q, v) = \sqrt{\frac{4Q}{\pi v}}$. The fluid rate further is a function of the process parameters including the operating pneumatic pressure, viscosity of the fluid, and the nozzle diameter.

One can imagine that the strut formation includes two processes: deposition material extrusion, and extruded deposition material cross-linking. The deposition material extrusion process is described by the analytic model, thus the involved parameters are examined: deposition flow rate; nozzle size and nozzle travel speed. The cross-linking process parameters are: alginate viscosity which regulates the ability of extruded material to hold the cylindrical shape during the cross-linking process; cross-linker concentration and cross-linker to deposition flow rate ratio those regulate the amount of cross-linker ions (calcium ions) available to alginate. During the examination of each parameter, the other parameters were set fixed while variant values of the examined parameter were tested to unveil the mere effect of the parameter on strut

formability. Since the cross-linker concentration and cross-linker to deposition flow rate ratio are dependent parameters, they were examined as pair combination. The examined values of the parameters were listed in Table 1. During the examination of the strut formability, the deposition material was selected as a mixture of the alginate product (1:3 as 71238: A0682). The strut size printed by each set of parameters was measured by optic microscope. Five samples for each set of parameter were examined. Mean strut size and standard deviation was calculated.

	Default value	Examined values
Deposition parameters:		
Deposition flow rate	23.56 mm^3/min	22.00, 23.56 and 26.00 mm^3/min
Nozzle size	250 um	200, 250 and 330 um
Nozzle travel speed	8 mm/s	4, 8 and 12 mm/s
Cross-linking parameters:		
Alginate concentration (viscosity)	4.5%	3%, 4.5% and 6%
Calcium concentration	5%	1%, 3% and 5%
Cross-linker to deposition flow rate ratio	3:1	1:1; 2:1; 3:1; 4:1; and 5:1

Table 1. Values examined in the strut formability study. Default values were the values used when another parameter was examined. Examined values were the set of values tested for the examining parameter.

Structural stability

Based on the result of the strut formability, the parametric values that succeeded to form the strut according to the analytic model were carried out for scaffold fabrication and stability examination. The stability study was designed to examine the capability of the scaffold to hold the structure against gentle fluidic disturbance.

Besides the deposition parameters and cross-linking parameters, the material composition was also examined. Two types of alginate products and the mixture of those with variant ratio were studied. The alginates were medium viscosity with high glucuronic acid content (71238) versus low viscosity with low glucuronic acid content (A0682). It was found that fabricated hydrogel scaffold structure with low viscosity and glucuronic acid alginate are more stable and able to sustain the structure against normal fluidic disturbance. However, when saturated within cell culture medium, the hydrogel structures would be degraded quickly. Conversely, hydrogel scaffold structure with medium viscosity and high glucuronic acid content are more resistant to degradation when saturated in cell culture medium, but the structure are less stable and very easy to fall apart under mild fluidic disturbance. Thus, the examination of the mixture with both products was proposed to determine the optimal mixture ratio for biomedical application. The examined values of parameters were listed in Table 2.

During the scaffold study, 3D hydrogel scaffolds were fabricated. Parallel strut pattern of 15 mm × 15 mm with 750 um between struts was designed and 10 perpendicular laid out layers were stacked to build the 3D scaffold. The elevation of each stack layer was set to be 0.2 mm. The scaffolds were then moved to 35 mm petri dish with DPBS immersed. A gentle fluidic

disturbance was introduced subsequently by orbital shaker of 100 rpm for 5 minutes. The structure before and after disturbance were compared for the examination of stability.

	Default value	Examined values
Deposition parameters:		
Deposition flow rate	23.56 mm^3/min	
Nozzle size	250 um	
Nozzle travel speed	8 mm/s	
Cross-linking parameters:		
Alginate concentration (viscosity)	4.5%	4.5% and 6%
Calcium concentration	5%	3% and 5%
Cross-linker to deposition flow rate ratio	3:1	2:1; 3:1; 4:1; and 5:1
Material composition:		
A0682: 71238	3:1	Pure A0682; 3:1; 2:1; 1:1 and pure 71238

Table 2. Values examined in the scaffold structurability and stability study. Default values were the values used when another parameter was examined. Examined values were the set of values tested for the examining parameter.

Structural integrity

The scaffolds that can sustain the structure from stability study were further examined for structural integrity study. The integrity study was intended to examine the capability of fabricated scaffold hold its structure in cell culture conditions. The scaffolds were immersed within cell culture medium (89% DMEM, 10% FBS, and 1% penicillin streptomycin) and incubated in 37 °C with 5% CO_2. Values examined for this study was listed in Table 3. The structure integrity was examined by checking the 3D structure at day 0, 1, 3, 5, 7, 9, 11, 13, 15.

	Default value	Examined values
Deposition parameters:		
Deposition flow rate	23.56 mm^3/min	
Nozzle size	250 um	
Nozzle travel speed	8 mm/s	
Cross-linking parameters:		
Alginate concentration (viscosity)	4.5%	4.5% and 6%
Calcium concentration	5%	3% and 5%
Cross-linker to deposition flow rate ratio	3:1	2:1; 3:1; 4:1; and 5:1
Material composition:		
A0682: 71238	3:1	Pure A0682; 3:1

Table 3. Values examined in the structural integrity study. Default values were the values used when another parameter was examined. Examined values were the set of values tested for the examining parameter.

Result

Strut formability

A set of parametric experimental studies were conducted to assess the effect of deposition parameters and cross-linking parameters on the strut formability. Fabricated struts were measured under optical microscope. Each data point was an average of five strut size fabricated with same set of parameters. The deposition parameters results were showed in Figure 2- 4, and the cross-linking parameters were showed in Figure 5, 6 and Table 4. Each of the experiment has one parameter examined to explore the effect of that parameter on strut formability and default values were used for the rest of the parameters. Since the cross-linker concentration and cross-linker to alginate flow rate ratio were dependent for cross-linker ions availability description, they were examined as pair combination.

From the results of strut formability study on deposition parameters, the developed analytic model can be verified. In the condition when sufficient cross-linking can be achieved, the strut size is predictable by the analytic model. Variation of the deposition parameter value would result in strut size change. The precision of the strut size can be achieved within 10 um using the proprietary in situ fabrication system.

The examination of cross-linking parameters showed that the strut formability is related to the cross-linking conditions. When the formability was examined as a function of alginate concentration, it can be found that expected strut size can be formed when the alginate concentration is higher than 4.5%. In the examination of strut formability as a function of cross-linker availability ($CaCl_2$ concentration and $CaCl_2$ to alginate flow rate ratio), the results showed that 1% calcium chloride cannot form expected strut size regardless the flow rate ratio utilized. The expected strut size can be achieved when the cross-linker to alginate flow rate ratio is higher than 3 when using 3% calcium chloride solution, and 2 when using 5% calcium chloride solution. As a summary of the cross-linker availability, strut formability of 4.5% concentration can be achieved within an appropriate cross-linking parameters range showed in figure 6D.

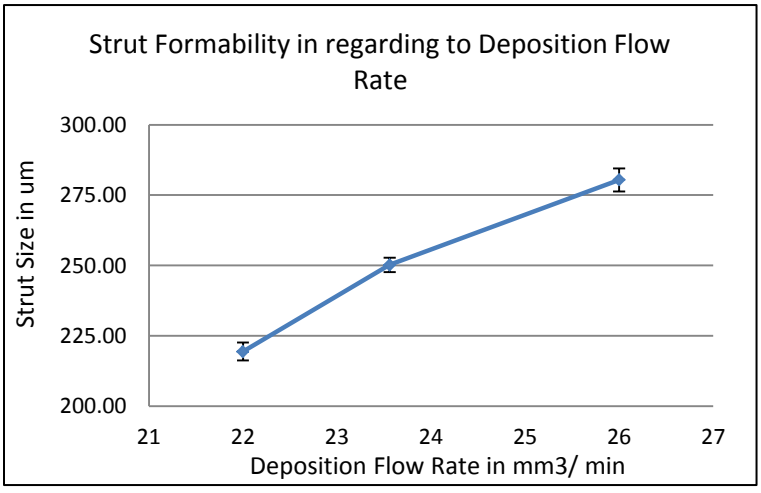

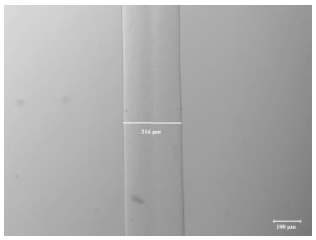

Flow rate: 22.00 mm^3/min
Strut Size: 216 um

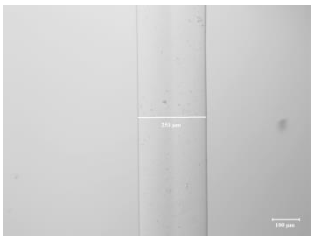

Flow rate: 23.56 mm^3/min
Strut Size: 253 um

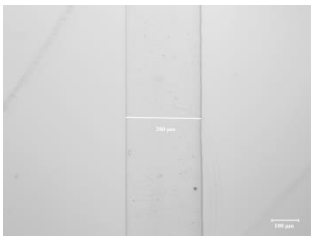

Flow rate: 26.00 mm^3/min
Strut Size: 280 um

Figure 2. Strut formability in regarding to deposition flow rate: the flow rate examined were 22.00 mm^3/min, 23.56 mm^3/min and 26.00 mm^3/min. The struts size were 219.40 um, 250.20 um and 280.40 um with standard error of 3.21 um, 2.59 um and 4.10 um respectively.

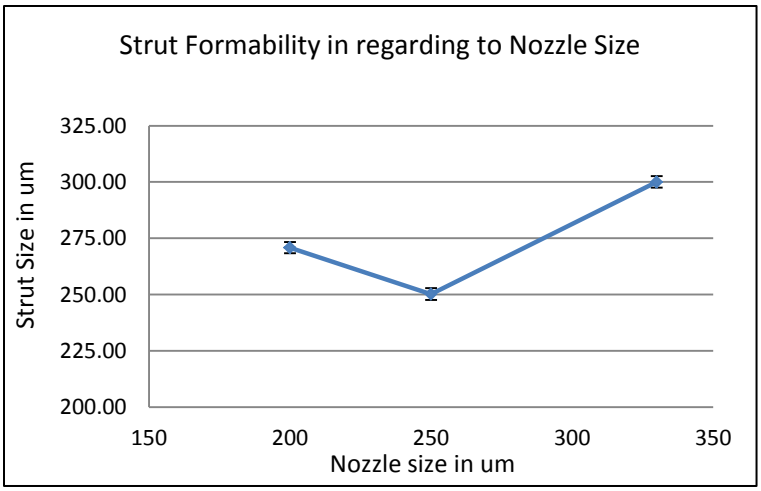

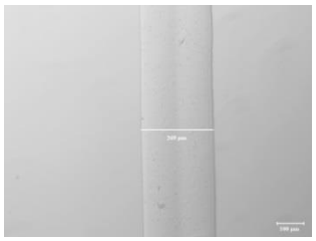

Nozzle Size: 200 um
Strut Size: 269 um

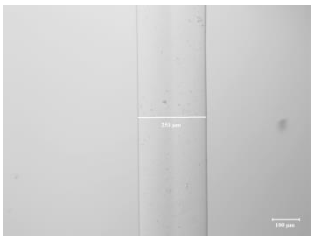

Nozzle Size: 250 um
Strut Size: 253 um

Nozzle Size: 330 um
Strut Size: 301 um

Figure 3. Strut formability in regarding to nozzle size: the nozzle size examined were 200 um, 250 um and 330 um. The strut size were 270.80 um, 250.20 um and 300.00 um with standard error of 2.49 um, 2.59 um and 2.55 um respectively.

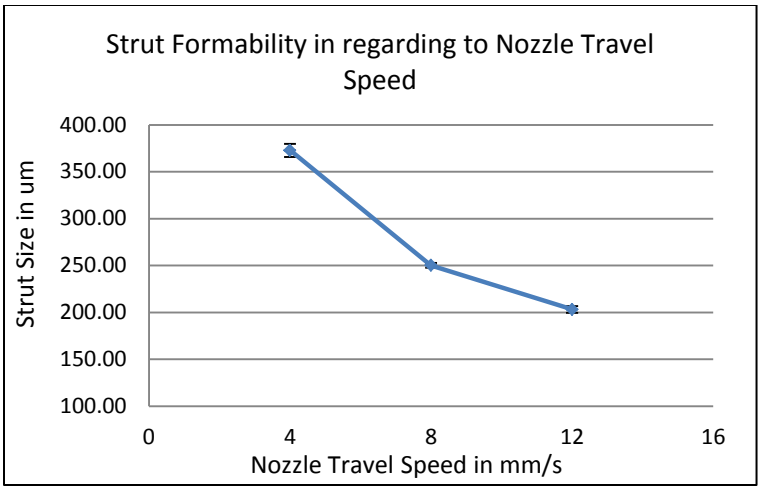

Nozzle Travel Speed: 4 mm/s
Strut Size: 371 um

Nozzle Travel Speed: 8 mm/s
Strut Size: 253 um

Nozzle Travel Speed: 12 mm/s
Strut Size: 202 um

Figure 4. Strut formability in regarding to nozzle travel speed: the nozzle travel speed examined were 4 mm/s, 8 mm/s and 12 mm/s. The strut size were 372.80 um, 250.20 um and 203.20 um with standard error of 7.05 um, 2.59 um and 3.56 um respectively.

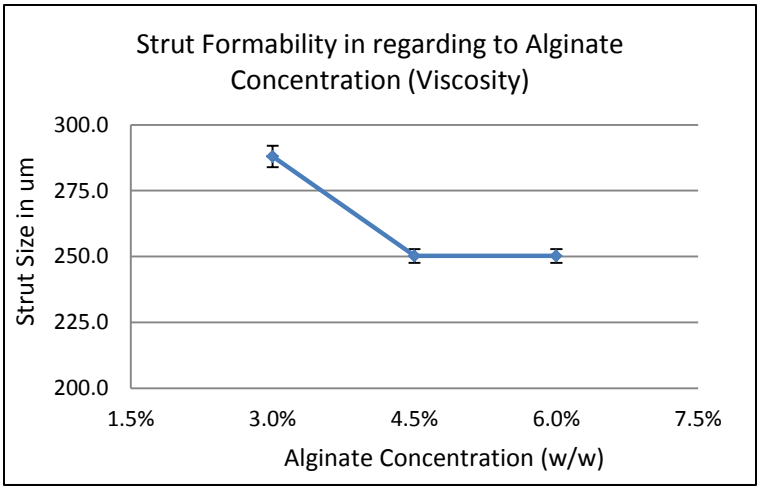

Alginate Concentration: 3.0%
Strut Size: 294 *um*

Alginate Concentration: 4.5%
Strut Size: 253 *um*

Alginate Concentration: 6.0%
Strut Size: 250 *um*

Figure 5. Strut formability in regarding to alginate concentration (viscosity): the alginate concentration examined were 3.0%, 4.5% and 6.0% (w/w). The strut size were 288 *um*, 250.20 *um* and 250.20 *um* with standard error of 4.06 *um*, 2.59 *um* and 2.59 *um* respectively.

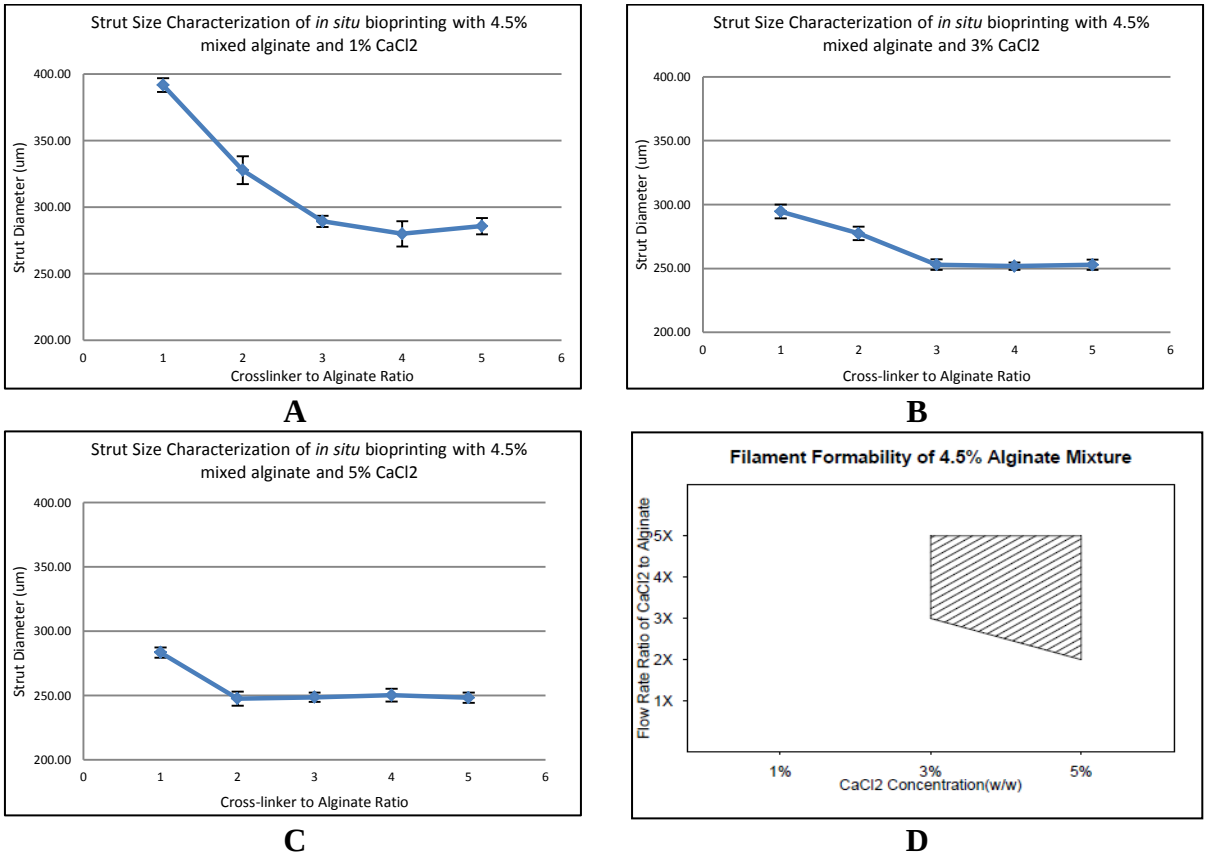

Figure 6. Strut size characterization as a function of $CaCl_2$ to alginate flow rate ratio in different $CaCl_2$ concentration (1%, 3% and 5% for **A**, **B** and **C** respectively). It can be summarized that the strut formability can be achieved within an appropriate cross-linking parameter range (shadow area in **D**).

Cross-linker concentration	Cross-linker to alginate flow rate ratio									
	1:1		2:1		3:1		4:1		5:1	
	Mean	SD	Mean	SD	Mean	SD	Mean	SD	Mean	SD

1%	391.8	5.22	327.8	10.47	289.4	4.16	280.0	9.41	285.8	6.06
3%	294.6	5.50	277.4	5.32	**253.0**	4.06	**251.8**	2.95	**252.8**	4.02
5%	283.4	4.04	**247.6**	5.50	**248.6**	3.58	**250.2**	4.97	**248.2**	3.96

Table 4. Strut formability in regarding to cross-linker availability ($CaCl_2$ concentration and $CaCl_2$ to alginate flow rate ratio): the $CaCl_2$ concentration examined were 1%, 3% and 5%; the $CaCl_2$ to alginate flow rate ratio examined were 1:1, 2:1, 3:1, 4:1 and 5:1. The results unit was um.

Structural stability

Parameter values that achieved strut formability (listed in Table 2.) were further utilized to fabricate the 3D porous laden structure (Figure 7.). Structural stability test were performed on the fabricated scaffolds. The structure before and after fluidic disturbance were showed in Figure 8- 10. From the observation, the fabricated scaffold would be able to hold its structure in both 4.5% and 6% alginate concentration that examined (Figure 8.). In material composition examination, the scaffold would be able hold the fluidic disturbance in the material composition of pure A0682 and 3:1 mixture (A0682 to 71238). The scaffolds fell apart in the material composition of 2:1, 1:1 mixture (A0682 to 71238) and pure 71238 (Figure 9.). When cross-linking process parameters were examined, all the scaffolds succeeded to sustain the scaffold structure against fluidic disturbance in the cross-linking range examined (Figure 10.).

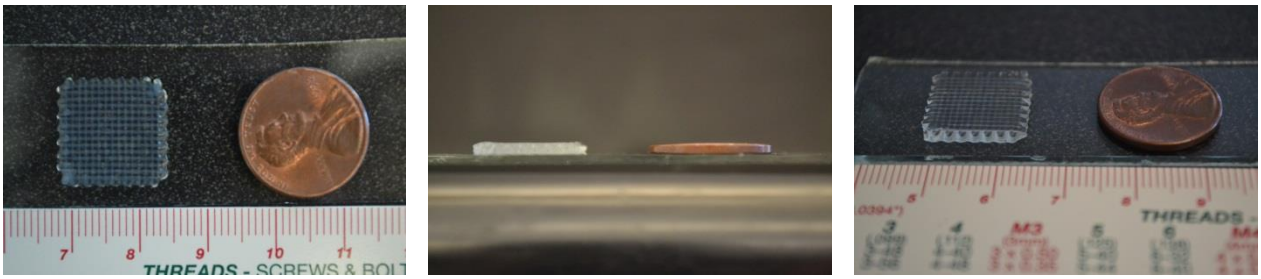

Top View Side View Angled View

Figure 7. 3D porous laden structure fabricated with *in situ* printing method using default fabrication parameters.

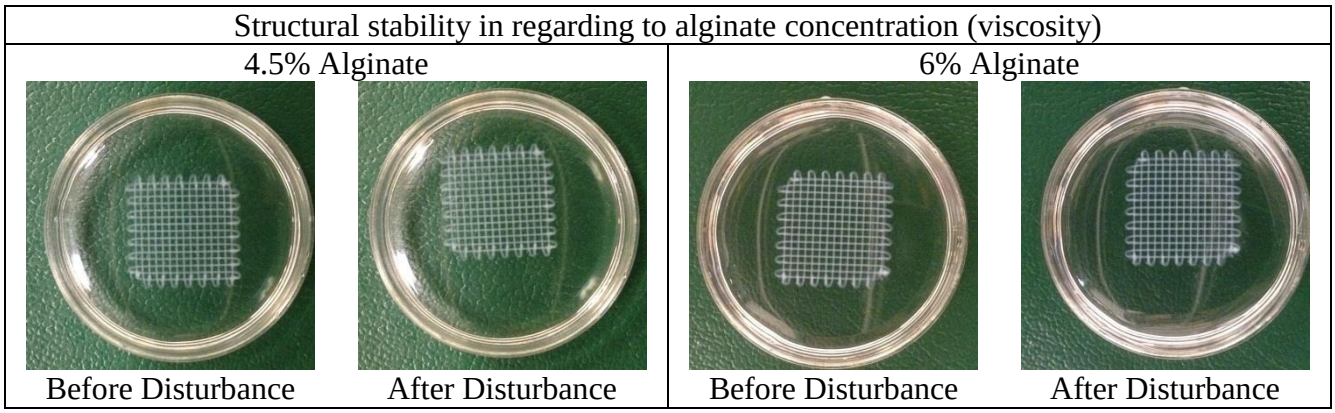

Figure 8. Structural stability in regarding to alginate concentration: the alginate concentration examined were 4.5% and 6% (w/w). The structures were stable in both alginate concentrations.

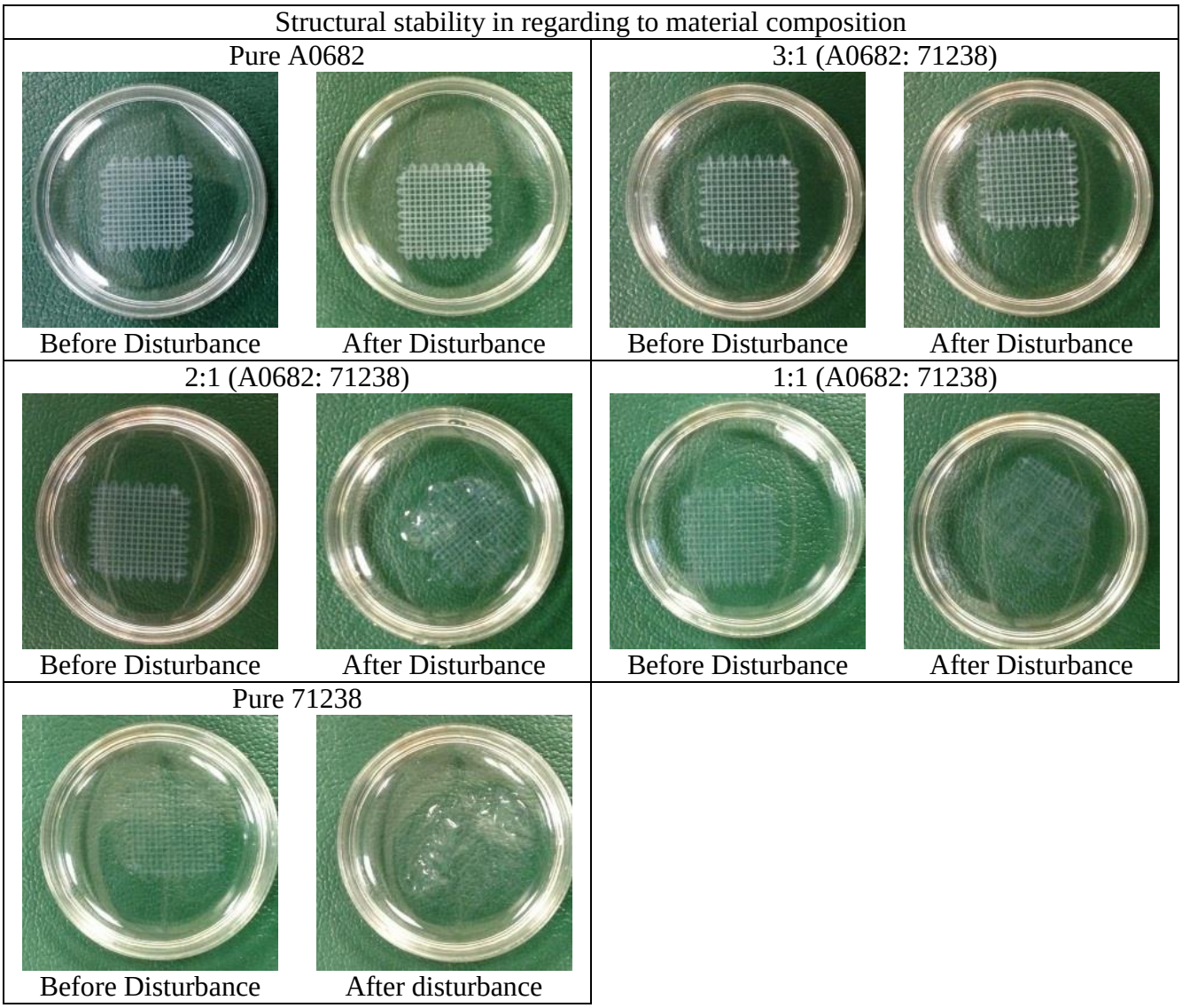

Figure 9. Structural stability in regarding to material composition: the material compositions examined were Pure A0682; 3:1; 2:1; 1:1 (A0682: 71238) and pure 71238. The structures were stable only in pure A0682 and 3:1 (A0682: 71238) material composition.

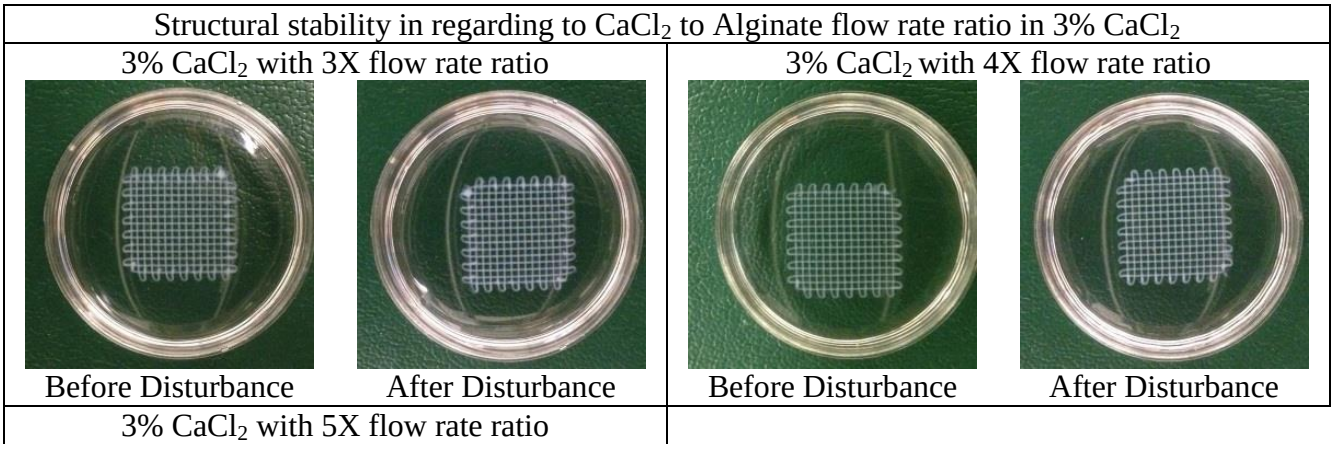

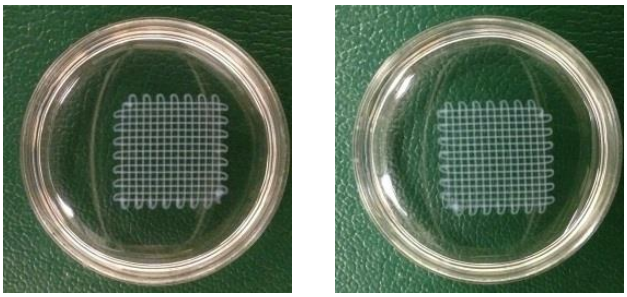

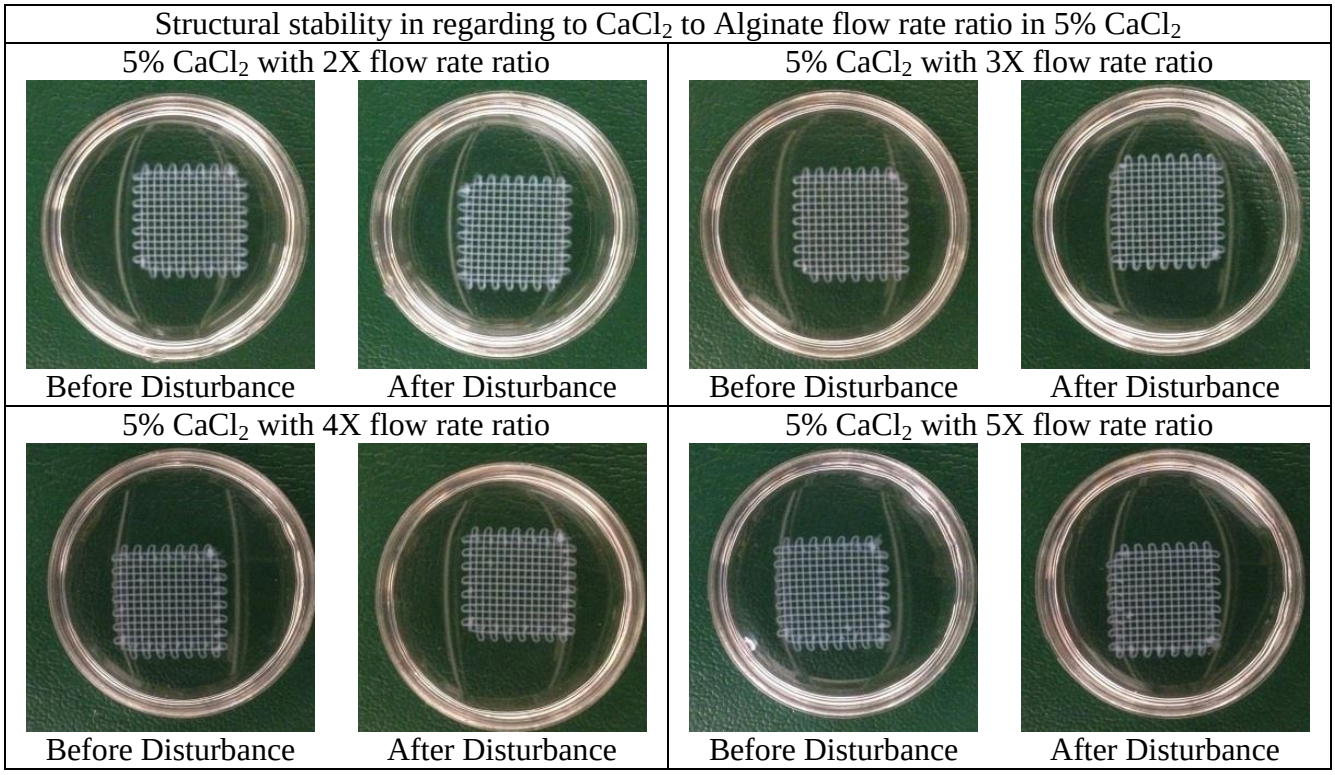

Figure 10. Structural stability in regarding to cross-linker availability ($CaCl_2$ concentration and $CaCl_2$ to alginate flow rate ratio): the examined $CaCl_2$ concentrations were 3% and 5%; the $CaCl_2$ to alginate flow rate ratios were 2:1; 3:1; 4:1 and 5:1. The structures were stable in all the cross-linker parameters.

Structural integrity

The fabricating parameters (Table 3.) that succeeded to form the strut and sustain the structure stability were further carried out for structural integrity. The scaffolds that incubated in cell culture medium were checked every two days from day 1 to day 15. From the observation, the fabricated scaffolds kept its structure when 3:1 (A0682: 71238) material composition was selected. The scaffolds that fabricated by pure A0682 was degraded out at day 3 (Figure 11.). There is no noticeable structure disturbance for other fabricating parameters when 3:1 (A0682: 71238) material composition was utilized.

Structural integrity in regarding to material composition
Pure A0682

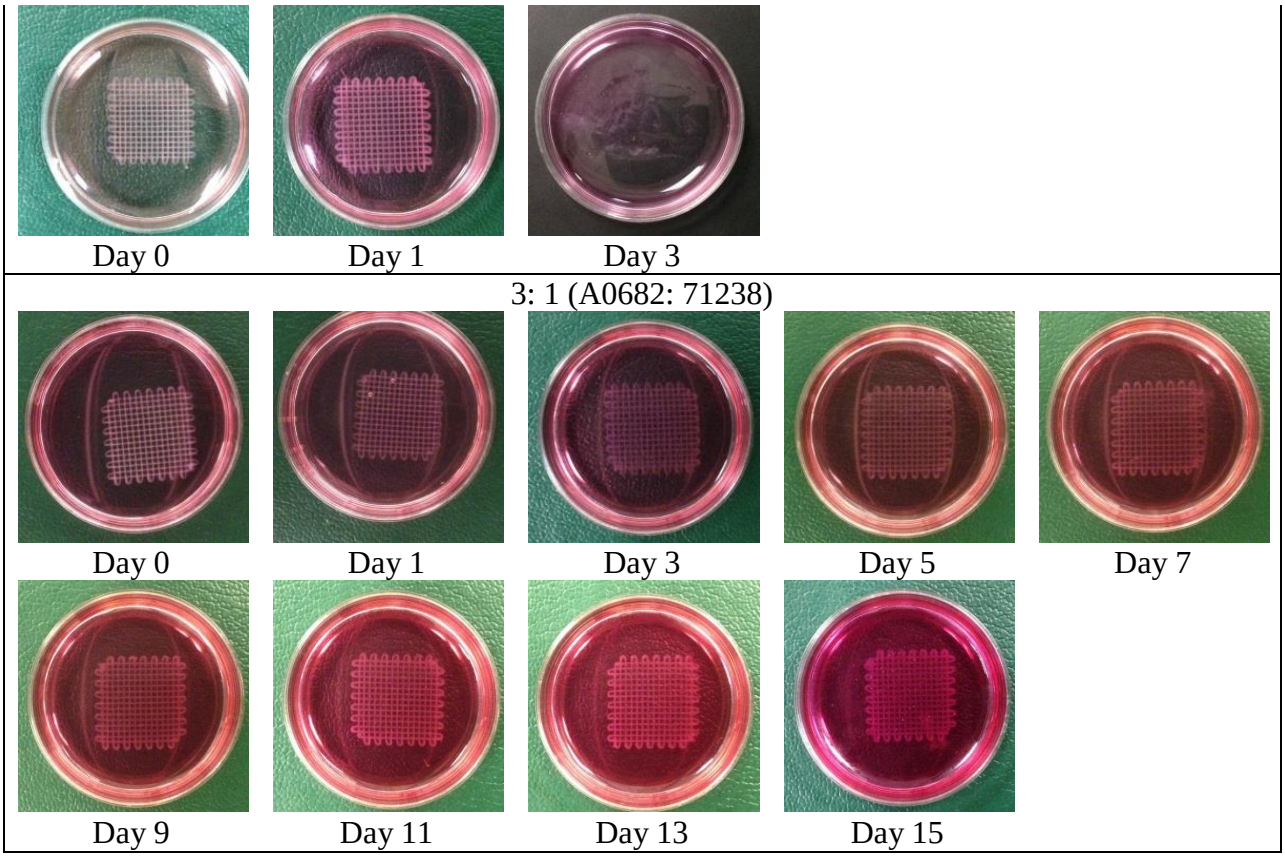

Figure 11. Structural integrity in regarding to material composition: The fabricated scaffolds were incubated in cell culture medium and checked from day 0 to day 15 every two days. Scaffold can hold its porous structure for 15 days when 3:1 (A0682: 71238) material composition was selected but degraded out at day 3 when pure A0682 was used.

Discussion

In the solid freeform fabrication-based *in situ* printing process, struts are first fabricated as basic element. A pattern of the struts were designed on each layer and were stacked together to form the porous 3D scaffold. To produce a porous scaffold with controllable structure feature and decent stability and integrity in cell culture environment, process parameter regarding to three structure characteristics – strut formability, structural stability and structural integrity, were examined.

Struts are the basic elements to build the 3D structures. The size of it determines the characteristics of the 3D porous laden structure fabricated (pore size, bio-component accessibility, degradation rate). The strut formation process involved the alginate deposing process and extruded alginate crosslinking process. From the examination of the deposing process parameters (deposition flow rate, nozzle size and travel speed), the strut formability agrees with the developed analytic model: $\mathrm{D} = f(Q, v) = \sqrt{\frac{4Q}{\pi v}}$. This result suggested that a cylindrical strut can be formed and limited swollen occurred in the fabrication process when cross-linkers are sufficient. When alternating one of the parameters, the strut will not form the expecting size. The cylindrical strut size agreed to the analytic model then is described as strut

formability achieved. In the examination of the crosslinking process parameters (alginate concentration, crosslinker concentration and crosslinker to deposition flow rate ratio), there is a critical minimum level for alginate concentration and crosslinker availability (crosslinker concentration and crosslinker to deposition flow rate ratio) to ensure the expected strut formation. The alginate concentration determines both the viscosity of the solution and crosslinking available alginate molecules concentration. The viscosity of the solution governs the spreading behavior of extruded alginate during the crosslinking process, and the crosslinking available alginate molecules concentration determines the stiffness of the strut. When alginate concentration is low, the extruded alginates are prone to spread during cross-linking and less stiff when cross-linked, thus failed to form the expected strut. In the consideration of cross-linker, the $CaCl_2$ concentration and flow rate ratio are dependent parameters both contribute to the cross-linker availability. Strut formability cannot be achieved using 1% Calcium Chloride or 1:1 flow rate ratio (cross-linker to alginate). This result suggested that when one of the parameter is too low, the cross-linker will not be sufficient regardless the other parameter. It also can be summarized from the results that there is a critical minimum combination of the two parameters. As the two parameters lied higher than the critical combination, strut formability can be achieved (Figure 6D). Thus, in the strut fabrication process, as the minimum crosslinking process sufficed, a strut can be fabricated based on a developed analytic model. Further, it can be observed that the printing system delivered a precise strut size within 10 um as formability achieved.

When examining cell behavior *in vitro*, it is essential that the *in vitro* model can stand decent fluidic disturbance when different biological assay were applied or fluidic flow that mimic the circulation system *in vivo* were applied. Similarly, cell reaction to stimulus is a time depending process, therefore a scaffold product that can sustain it structure within a decent time frame is necessary. To render a scaffold product with decent stability and integrity in cell culture environment, the structural stability and integrity studies were performed. From the results of the two studies, the stability and integrity was only affected by the alginate composition. Two different types of alginate were selected and mixed in different ratios as the parameter of alginate composition. Scaffold fabricated using alginate with low viscosity and low glucuronic acid content (A0682) was found more stable as structure against fluidic disturbance but degraded quickly in cell culture environment. The product with medium viscosity and high glucuronic acid content (71238) can hold its structure longer in cell culture environment but less stable against gentle fluidic disturbance. The mixture ratio of 1:3 (71238 to A0682) delivered the scaffold product with decent stability and integrity.

Reference

[1] R. Langer and J. P. Vacanti, "Tissue Engineering," *Science,* vol. 260, pp. 920-926, May 14 1993.

[2] Y. L. Cao, J. P. Vacanti, K. T. Paige, J. Upton, and C. A. Vacanti, "Transplantation of chondrocytes utilizing a polymer-cell construct to produce tissue-engineered cartilage in the shape of a human ear," *Plastic and Reconstructive Surgery,* vol. 100, pp. 297-302, Aug 1997.

[3] W. C. Puelacher, J. Wisser, C. A. Vacanti, N. F. Ferraro, D. Jaramillo, and J. P. Vacanti, "Temporomandibular-Joint Disc Replacement Made by Tissue-Engineered Growth of Cartilage," *Journal of Oral and Maxillofacial Surgery,* vol. 52, pp. 1172-1177, Nov 1994.

[4] Y. L. Weng, Y. L. Cao, C. A. Silva, M. P. Vacanti, and C. A. Vacanti, "Tissue-engineered composites of bone and cartilage for mandible condylar reconstruction," *Journal of Oral and Maxillofacial Surgery,* vol. 59, pp. 185-190, Feb 2001.

[5] C. Ibarra, C. Jannetta, C. A. Vacanti, Y. Cao, T. H. Kim, J. Upton, *et al.*, "Tissue engineered meniscus: A potential new alternative to allogeneic meniscus transplantation," *Transplantation Proceedings,* vol. 29, pp. 986-988, Feb-Mar 1997.

[6] K. Kojima, L. J. Bonassar, R. A. Ignotz, K. Syed, J. Cortiella, and C. A. Vacanti, "Comparison of tracheal and nasal chondrocytes for tissue engineering of the trachea," *Annals of Thoracic Surgery,* vol. 76, pp. 1884-1888, Dec 2003.

[7] H. Mizuno, A. K. Roy, C. A. Vacanti, K. Kojima, M. Ueda, and L. J. Bonassar, "Tissue-engineered composites of anulus fibrosus and nucleus pulposus for intervertebral disc replacement," *Spine,* vol. 29, pp. 1290-1297, Jun 15 2004.

[8] S. H. Kamil, K. Kojima, M. P. Vacanti, L. J. Bonassar, C. A. Vacanti, and R. D. Eavey, "In vitro tissue engineering to generate a human-sized auricle and nasal tip," *Laryngoscope,* vol. 113, pp. 90-94, Jan 2003.

[9] W. C. Puelacher, D. Mooney, R. Langer, J. Upton, J. P. Vacanti, and C. A. Vacanti, "Design of Nasoseptal Cartilage Replacements Synthesized from Biodegradable Polymers and Chondrocytes," *Biomaterials,* vol. 15, pp. 774-778, Aug 1994.

[10] W. C. Puelacher, J. P. Vacanti, N. F. Ferraro, B. Schloo, and C. A. Vacanti, "Femoral shaft reconstruction using tissue-engineered growth of bone," *International Journal of Oral and Maxillofacial Surgery,* vol. 25, pp. 223-228, Jun 1996.

[11] C. A. Vacanti, L. J. Bonassar, M. P. Vacanti, and J. Shufflebarger, "Replacement of an avulsed phalanx with tissue-engineered bone.," *New England Journal of Medicine,* vol. 344, pp. 1511-1514, May 17 2001.

[12] K. Arai, S. Iwanaga, H. Toda, C. Genci, Y. Nishiyama, and M. Nakamura, "Three-dimensional inkjet biofabrication based on designed images," *Biofabrication,* vol. 3, Sep 2011.

[13] M. Nakamura, A. Kobayashi, F. Takagi, A. Watanabe, Y. Hiruma, K. Ohuchi, *et al.*, "Biocompatible inkjet printing technique for designed seeding of individual living cells," *Tissue Engineering,* vol. 11, pp. 1658-1666, Nov 2005.

[14] D. J. Odde and M. J. Renn, "Laser-guided direct writing of living cells," *Biotechnology and Bioengineering,* vol. 67, pp. 312-318, Feb 5 2000.

[15] L. Koch, S. Kuhn, H. Sorg, M. Gruene, S. Schlie, R. Gaebel, *et al.*, "Laser Printing of Skin Cells and Human Stem Cells," *Tissue Engineering Part C-Methods,* vol. 16, pp. 847-854, Oct 2010.

[16] D. L. Cohen, E. Malone, H. Lipson, and L. J. Bonassar, "Direct freeform fabrication of seeded hydrogels in arbitrary geometries," *Tissue Engineering,* vol. 12, pp. 1325-1335, May 2006.
[17] S. Ahn, H. Lee, J. Puetzer, L. J. Bonassar, and G. Kim, "Fabrication of cell-laden three-dimensional alginate-scaffolds with an aerosol cross-linking process," *Journal of Materials Chemistry,* vol. 22, pp. 18735-18740, 2012.
[18] S. Khalil and W. Sun, "Bioprinting Endothelial Cells With Alginate for 3D Tissue Constructs," *Journal of Biomechanical Engineering-Transactions of the Asme,* vol. 131, Nov 2009.
[19] S. Ahn, H. Lee, E. J. Lee, and G. Kim, "A direct cell printing supplemented with low-temperature processing method for obtaining highly porous three-dimensional cell-laden scaffolds," *Journal of Materials Chemistry B,* vol. 2, pp. 2773-2782, 2014.
[20] Y. Zhao, R. Yao, L. L. Ouyang, H. X. Ding, T. Zhang, K. T. Zhang, *et al.*, "Three-dimensional printing of Hela cells for cervical tumor model in vitro," *Biofabrication,* vol. 6, Sep 2014.